

Molecular analysis of rugosity in a *Vibrio cholerae* O1 El Tor phase variant

Fitnat H. Yildiz,^{1*} Xiaole S. Liu,² Arne Heydorn³ and Gary K. Schoolnik⁴

¹Department of Environmental Toxicology, University of California, Santa Cruz, 269 Jack Baskin Engineering Bldg, Santa Cruz, CA 95064, USA.

²Department of Biostatistical Sciences, Harvard School of Public Health, Dana-Farber Cancer Institute, 44 Binney St., Mayer 1B22, Boston, MA 02115, USA.

³Department of Pharmacology, University of Copenhagen, The Panum Institute, 18.6 Blegdamsvej 3, DK-2200 Copenhagen, Denmark.

⁴Department of Medicine, Division of Infectious Diseases and Geographic Medicine, and Department of Microbiology and Immunology, Stanford University Medical School, Beckman Center, Room 239, Stanford, CA 94305, USA.

Summary

Reversible phase variation between the rugose and smooth colony variants is predicted to be important for the survival of *Vibrio cholerae* in natural aquatic habitats. Microarray expression profiling studies of the rugose and smooth variants of the same strain led to the identification of 124 differentially regulated genes. Further expression profiling experiments showed how these genes are regulated by the VpsR and HapR transcription factors, which, respectively, positively and negatively regulate production of VPS^{El Tor}, a rugose-associated extracellular polysaccharide. The study of mutants of *rpoN* and *rpoS* demonstrated the effects of these alternative sigma factors on phase variation-specific gene expression. Bioinformatics analysis of these expression data shows that 'rugosity' and 'smoothness' are determined by a complex hierarchy of positive and negative regulators, which also affect the biofilm, surface hydrophobicity and motility phenotypes of the organism.

Introduction

Vibrio cholerae, the aetiological agent of Asiatic cholera, is also a natural inhabitant of aquatic environments (Islam

et al., 1993; Faruque *et al.*, 1998). In habitats of this kind, *V. cholerae* has been hypothesized to switch between the smooth and rugose colony morphotypes, a capacity that was proposed by Balteanu in 1926 and by White in 1938 to contribute to its environmental survival (White, 1938). However, the rugose phase variant was very little studied until the recent cholera epidemic in Peru, where traits associated with rugosity were found to increase the survival of *V. cholerae* in chlorinated water (Rice *et al.*, 1992; Morris *et al.*, 1996). Morris *et al.* (1996) subsequently showed that the rugose variant can cause cholera in orally challenged human volunteers and retains its colonial morphology after passage through the human host. The rugose colony morphotype has also been isolated from the stools of naturally infected cholera patients and from environmental biofilm samples in Bangladesh (Dr M. S. Islam, International Center for Diarrhoeal Disease Research, Dhaka, Bangladesh, personal communication). More recent studies have shown that epidemic strains of *V. cholerae* switch from the smooth to the rugose phase more frequently than clinical isolates (Ali *et al.*, 2002), and that this phase transition increases the resistance of the organism to osmotic, acid and oxidative stress and enhances its capacity to form a biofilm (Wai *et al.*, 1998; Yildiz and Schoolnik, 1999; Watnick *et al.*, 2001). The latter property is associated with increased production of *Vibrio* polysaccharide (VPS^{ETr}) by the rugose variant of the El Tor biotype (Yildiz and Schoolnik, 1999). Further examination of this association showed that VPS^{ETr} is directly responsible for many of the phenotypic properties of the rugose variant (Yildiz and Schoolnik, 1999).

The genes required for VPS^{ETr} synthesis, identified through transposon mutagenesis, were designated *vps* for *Vibrio* polysaccharide and shown to be clustered in two regions in a 30.7 kb segment on the large chromosome of *V. cholerae* O1 El Tor (Yildiz and Schoolnik, 1999). A positive transcriptional regulator of *vps* gene expression, denoted *vpsR* (*Vibrio* polysaccharide regulator), was also identified by transposon mutagenesis (Yildiz *et al.*, 2001). VpsR exhibits homology to the NtrC subclass of two-component response regulators. Disruption of *vpsR* in the rugose phase variant genetic background yields the smooth colony morphotype, prevents expression of *vpsA* and *vpsL* and production of VPS^{ETr} and abolishes formation of typical three-dimensional biofilms (Yildiz *et al.*,

Accepted 31 March, 2004. *For correspondence. E-mail yildiz@etox.ucsc.edu; Tel. (+1) 831 459 1588; Fax (+1) 831 459 3524.

2001), demonstrating that VpsR positively regulates the manifestation of rugosity-associated phenotypes.

HapR, a positive regulator of *hap* haemagglutinin/protease (HA/P) expression, represses the rugose colony morphotype in the smooth colonial variant (Jobling and Holmes, 1997). Moreover, recent studies show that it negatively regulates biofilm formation through its role in a quorum-sensing signal transduction system (Zhu *et al.*, 2002; Hammer and Bassler, 2003; Zhu and Mekalanos, 2003).

With the availability of the completely sequenced genome of *V. cholerae* O1 El Tor, we used a genome-wide approach to understand the nature of smooth-to-rugose phase variation. To this end, we performed whole-genome expression profiling studies of smooth and rugose phase variants and of the *vpsR* and *hapR* mutants in each of the two (smooth or rugose) genetic backgrounds. Because VpsR belongs to the NtrC subclass of response regulators, which act in concert with alternative sigma factor RpoN, expression profiling studies were also conducted with *rpoN* mutants in each of the genetic backgrounds. Similarly, because the stationary phase alternative sigma factor RpoS was previously reported to positively regulate production of HA/P (Yildiz and Schoolnik, 1998), thus suggesting that RpoS augments *hapR* expression or influences its function as a transcription factor, microarray expression profiling studies were also used to compare the smooth RpoS mutant with the smooth phase variant of the wild-type parent. Together, these results show that 'smoothness' and 'rugosity' are the consequence of an interplay between positive and negative regulators of smooth-to-rugose phase variation genes. An unanticipated result of these expression profiling studies was elucidation of the role of *rpoN* and *rpoS* in regulating the expression of major pathogenicity genes through their regulation of *hapR*.

Results and discussion

Genomic analysis of the smooth and rugose colonial variants

The smooth and rugose colony variants of *V. cholerae* O1 El Tor differ markedly in appearance, biofilm development and architecture, and resistance to osmotic, acid and oxidative stress. To learn more about the molecular basis for these phenotypes and the nature of smooth-to-rugose phase variation, whole-genome expression profiles of the smooth and rugose phase variants during exponential growth (OD₆₀₀ 0.3–0.4) in LB broth were compared. The gene expression data were analysed by the statistical analysis of microarray (SAM) program (Tusher *et al.*, 2001) using the following criteria to define significantly regulated genes: $\leq 1\%$ false-positive discovery rate and

≥ 1.5 -fold transcript abundance differences between the samples. These criteria led to the identification of 124 genes that were differentially regulated in the smooth compared with the rugose phase variant of the same strain during exponential growth in liquid LB medium. Of these, 77 were induced and 47 repressed in the rugose compared with the smooth variant (Fig. 1A). In this and subsequent sections, these 124 genes are operationally defined to comprise the smooth-to-rugose phase variation regulated gene set, henceforth denoted S/R-*pvr*. Based on annotated functions provided by the *V. cholerae* genome sequencing project (Heidelberg *et al.*, 2000), the S/R-*pvr* genes are predicted to participate in a variety of cellular functions. The complete list of differentially regulated genes is provided in *Supplementary material*, Appendix S1. Below, we discuss a selected subset of these genes.

The hallmark of rugosity is the corrugated colonial morphotype, which is thought to be mediated in part by increased production of VPS^{EITor} (Yildiz and Schoolnik, 1999). Analysis of the expression profiles of the two wild-type phase variants supported this idea because the expression of most of the previously identified *vps* genes – VC0916, VC0917–VC0928 and VC0934–VC0939 – which are believed to encode proteins required for exopolysaccharide biosynthesis, was markedly induced in the rugose colonial variant. Genes located in the *vpsI* operon (VC0917–VC0928) were induced 3.7- to 6.3-fold (Fig. 1A and B), and genes in the *vpsII* operon (VC0934–VC0938) were induced 7.9- to 20-fold (Fig. 1A and C) compared with their expression in the smooth variant. In contrast, the transcript abundance of VC0939, the last gene in the six-gene *vpsII* operon, was considerably lower, only 1.59-fold greater in the rugose compared with the smooth variant. Taken together, these results show that, on average, *vpsII* operon genes are more strongly expressed than genes in the *vpsI* operon, a finding that points to a possible difference in how the two *vps* operons are regulated.

Microarray expression results also revealed that five genes within the *vps* cluster, which are not predicted to encode polysaccharide biosynthetic enzymes, were also significantly induced in the rugose variant (Fig. 1A). These include VC0930 (encoding a haemolysin-like protein) and VC0928, VC0929, VC0931 and VC0932 (encoding hypothetical proteins). In bacteria, genes that participate in the same biosynthetic or metabolic pathway tend to be clustered together on the chromosome. At present, it is not known whether all the genes in the *vps* region are required for the synthesis/export of VPS^{EITor} and the development of the rugose colony morphotype. However, evidence in support of this possibility comes from Ali *et al.* (2000a), who reported that a Tn5::*phoA* insertion into VC0930 led to the conversion of the rugose to a smooth

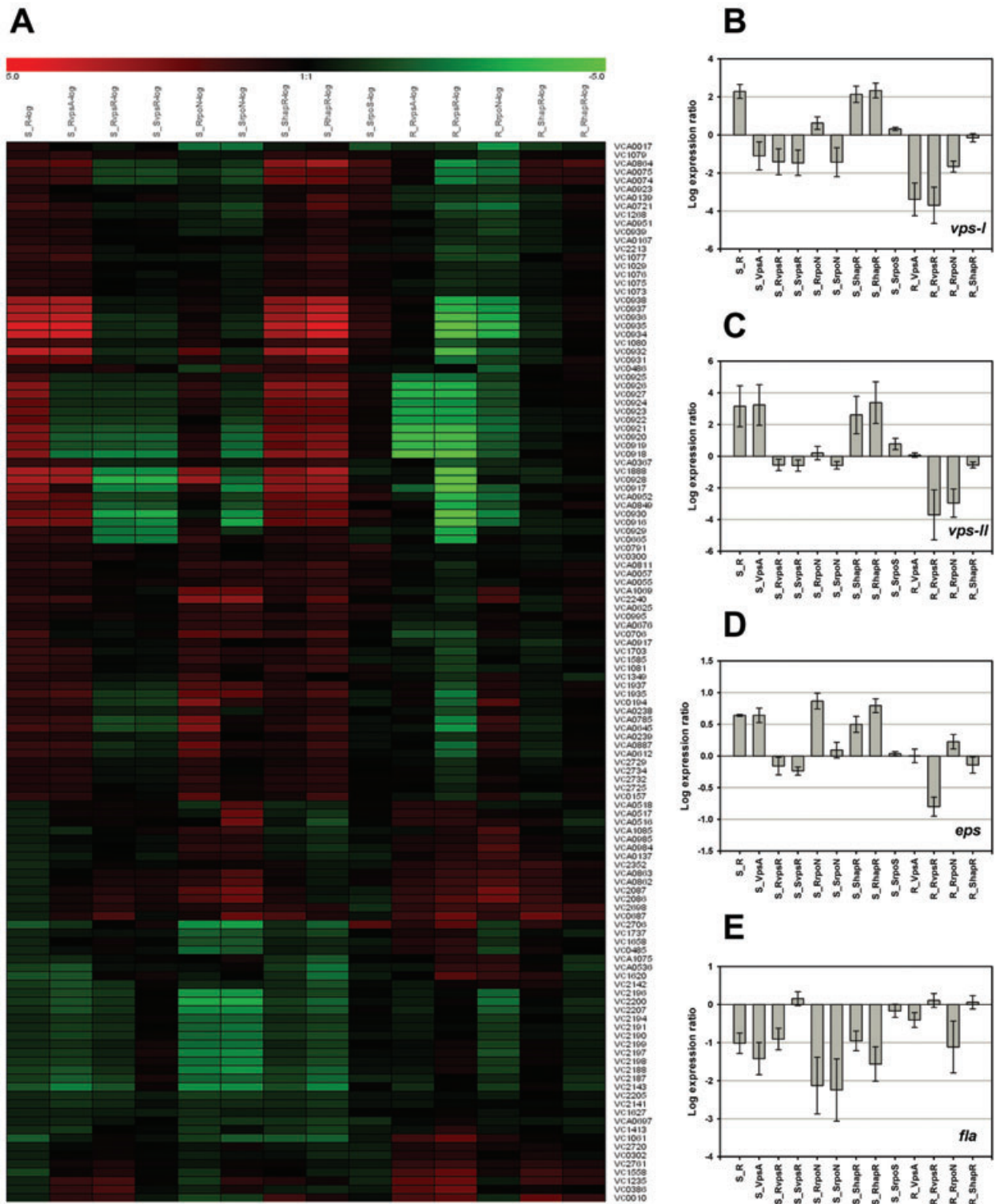


Fig. 1. Cluster analysis of S/R *pvr* genes and their dependence on regulatory genes. Smooth to rugose phase variation-regulated genes are identified by SAM analysis of whole-genome expression profiles of the exponentially grown phase variants. The S/R *pvr* genes are clustered via hierarchical clustering (A). Each comparison is represented by a single column, and the expression profile of each gene is represented in rows. Expression ratios are presented according to a colour scale shown at the top. Average induction or repression values for the *vpsI* cluster (B), *vpsII* cluster (C), *eps* genes (D) and *fla* (E) for each phase variant and mutant are presented.

colonial morphotype. Thus, although VC0930 is annotated as a haemolysin-like protein, this finding suggests that it is required for rugose colony formation. In addition to VC0930, analysis of the rugose colonial variant expression profile showed increased mRNA levels of another gene predicted to encode a haemolysin-related protein (VC1888). This gene has not been mutationally inactivated and, thus, its role in VPS^{EITor} synthesis or rugose colony development is unknown

Exopolysaccharide production requires activated sugar nucleotide intermediates (Nesper *et al.*, 2001). Expression of *galU* (VC0395), encoding for UDP-glucose pyrophosphorylase, which catalyses the production of UDP-glucose, is increased in the rugose variant by 1.6-fold relative to the smooth variant in colonies formed after 24 h incubation on LB agar at 30°C (data not shown). Furthermore, mutational analysis showed that *galU* is required for rugose colonial morphology (Nesper *et al.*, 2001). It has been reported that mutation of *galE*, which encodes for UDP-galactose epimerase, also renders the rugose variant smooth (Nesper *et al.*, 2001). However, the expression of *galE* was not different between the phase variants. These studies altogether indicate that the synthesis of activated sugar nucleotide intermediates and, in turn, the distribution of carbon between catabolism and biosynthesis is likely to be different between the two colonial variants.

The expression of four of the 15 *eps* (extracellular protein secretion) genes, located in a 12-gene operon containing *epsC–epsN*, was increased ≥ 1.5 -fold in the rugose phase variant (Fig. 1A and D). This observation is congruent with the report by Ali *et al.* (2000b) showing that two products of the Eps pathway (encoded by *epsD* and *epsE*) are required for the formation of the rugose colonial morphotype. This type II secretion system is also required for the secretion of proteins through the outer membrane including cholera toxin (CT), HA/P, chitinase, neuraminidase and lipase (Sandkvist, 2001a,b). However, it is not clear whether mutations in this pathway cause loss of rugosity because they prevent VPS^{EITor} secretion or because they prevent the secretion of protein(s) involved in the transport/assembly of VPS^{EITor}.

The expression of VC1073 and VCA0811, both annotated to encode putative chitinases, and VC0995, encoding the *N*-acetyl glucosamine-specific IIABC component NagE, was increased in the rugose variant. Motif analysis of the predicted protein products of VC1073 and VCA0811 showed that the latter chitinase homologue lacks the catalytic domain but has retained a chitin-binding domain and, consequently, is predicted to bind, but not degrade, chitin. In contrast, VC1073 is predicted to encode a chitin-hydrolysing protein. Glycosyl composition analysis of VPS^{EITor} showed *N*-acetyl glucosamine (GlcNAc) to be a component of this polysaccharide (Yildiz and Schoolnik,

1999). As chitin is a polymer of GlcNAc, we speculate that VPS^{EITor}, produced by the rugose phase variant, might be hydrolysed by the chitinase encoded by VC1073 and the resulting oligosaccharides, including GlcNAc, used as a carbon and nitrogen source. If so, then it seems possible that this chitinase might also promote detachment of *V. cholerae* from a biofilm matrix composed of VPS^{EITor}. This possibility is particularly intriguing because, in contrast to the four other *V. cholerae* genes annotated to encode chitinases, only VC1073 is not induced during growth on a chitin surface or in media containing soluble chitin oligosaccharides (Meibom *et al.*, 2004).

Phase variation-dependent differences in the production or modification of VPS^{EITor} are expected to influence biofilm development and structure. To test this idea, we compared the biofilm-forming capacities of the smooth and rugose phase variants by crystal violet staining of the biofilms formed on microtitre plates after 6 h of incubation under static conditions at 30°C. The results, shown in Fig. 2A, confirmed previous reports that the rugose variant forms a more substantial biofilm than the smooth variant (Yildiz and Schoolnik, 1999). To gain insight into the structure of biofilms formed by the phase variants under non-static conditions, biofilms were grown at 30°C in flow chambers and analysed by confocal scanning laser microscopy (CSLM) (Heydorn *et al.*, 2000a,b). In contrast to the biofilm phenotypes observed under static conditions of growth, both smooth and rugose variants were able to form very well-developed biofilms with characteristic three-dimensional, pillar-like structures (Fig. 2B). One likely explanation for the improved capacity of the smooth variant to form well-developed biofilms under flow conditions could be the limited accumulation of quorum signals under this growth condition because *V. cholerae* biofilm formation is negatively regulated by quorum signals (Zhu *et al.*, 2002; Hammer and Bassler, 2003; Zhu and Mekalanos, 2003).

Quantitative analysis of these biofilm images was performed with COMSTAT (Heydorn *et al.*, 2000b) and disclosed important differences between the two biofilms (Fig. 2C): the average thickness of rugose biofilms was greater (35 μm) compared with smooth biofilms (25 μm); and surface roughness, a measure of biofilm heterogeneity that indicates how biofilm thickness varies, was greater for rugose compared with smooth biofilms, indicating that the surface architecture of rugose biofilms is more irregular (Heydorn *et al.*, 2000b). In contrast, substratum coverage, which is a measure of the percentage of the surface that is covered by the bacteria at the substratum, was similar between the smooth and rugose phase variants.

In addition to differences in colony morphotype and biofilm phenotype, the smooth and rugose phase variants were also found to exhibit differences in surface hydropho-

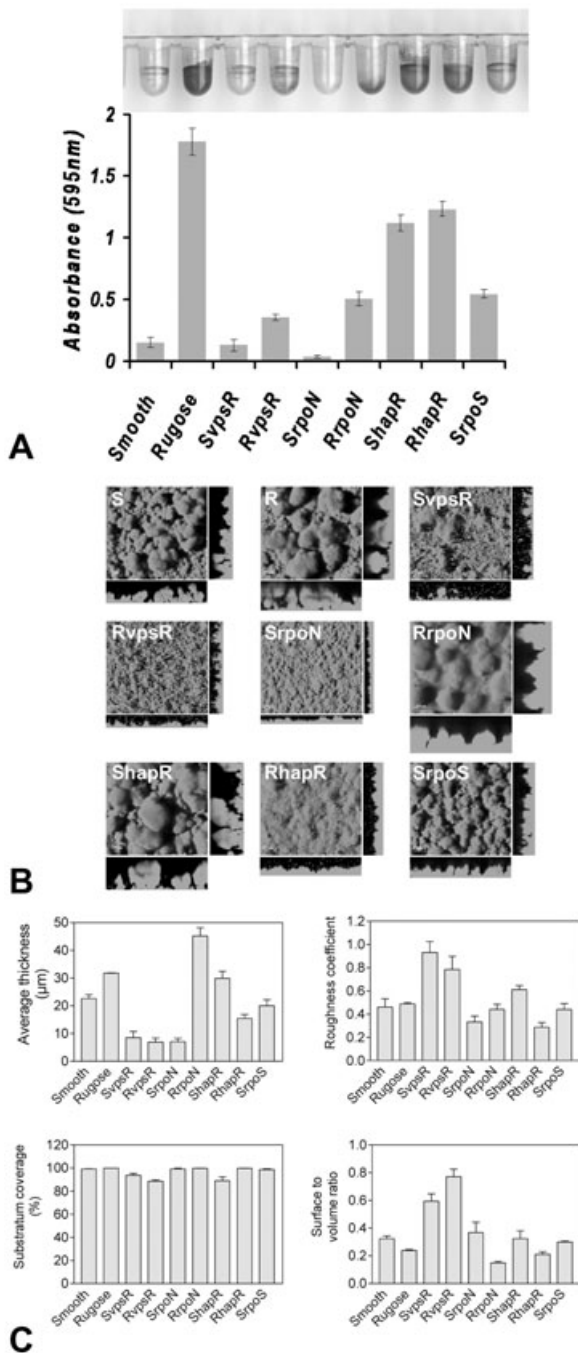


Fig. 2. Biofilm phenotypes of phase variants and regulatory mutants. **A.** Analysis of biofilms formed under static conditions. Biofilms were quantified for each strain by growing them overnight in LB broth at 30°C in polyvinyl chloride microtitre plates. The wells were washed after 6 h of incubation under static conditions, the attached bacteria were stained with crystal violet, and the staining intensity was monitored by absorbance of ethanol-solubilized stained films at 595 nm. **B.** Biofilm structures of phase variants and regulatory mutants. Biofilms were formed in flow chambers, and images were acquired via CSLM. Large panels represent a top-down view of the biofilms, and side panels represent a vertical view. **C.** Analysis of biofilm structures. Average thickness, roughness, substratum coverage and surface to volume ratio of 24-h-old biofilms of *V. cholerae* strains were quantified by the computer program COMSTAT.

bicity as determined by the direction-of-spreading (DOS) method (Rosenberg and Doyle, 1990). This assay showed that the rugose variant is dramatically more hydrophobic than the smooth variant (Table 1). This property can be attributed to increased production of VPS^{EITor} by the rugose variant as the colonial hydrophobicity of a *vpsA* mutant in the rugose genetic background is similar to that of the smooth variant. The compositional analysis of VPS^{EITor} showed that it is only 30% polysaccharide by weight (Yildiz and Schoolnik, 1999), a finding that suggests that it could contain acetate, pyruvate or succinate – common constituents of bacterial exopolysaccharides (Jansson *et al.*, 1975) that would increase the hydrophobicity of the compound.

The rugose variant exhibits increased resistance to chlorine and to hydrogen peroxide (Rice *et al.*, 1992; Wai *et al.*, 1998). The first of these properties clearly resides in VPS^{EITor} and its capacity to inactivate chlorine (Yildiz and Schoolnik, 1999). However, the chemical basis for the resistance of the rugose variant to H₂O₂ is unknown. Thus, it was of considerable interest to find, within the expression profile of the wild-type rugose variant, an increase in expression of VC1585, which encodes for catalase (KatB). This finding suggests that the increased expression of catalase by the rugose variant explains its increased resistance to H₂O₂, but does not explain how or why this oxidative stress response is upregulated in this colonial variant. However, from an evolutionary and ecological perspective, this response may be highly adaptive as biofilms containing the rugose variant that form in the photic zone of the water column are likely to be exposed to H₂O₂, generated by the UV irradiation of water (Arana *et al.*, 1992).

Comparison of whole-genome expression profiles of the smooth and rugose phase variants during exponential phase growth revealed marked differences in the transcription of some genes required for flagellar biosynthesis (VC2141, VC2142, VC2143, VC2187, VC2188, VC2190, VC2191, VC2194, VC2196, VC2197, VC2198, VC2199, VC2200).

Genes encoding flagellar components are located in six different regions and organized into 18 different transcriptional units on the large chromosome (Prouty *et al.*, 2001). A hierarchical transcriptional arrangement controlling flagellar gene expression in *V. cholerae* has been proposed (Prouty *et al.*, 2001). According to this model, flagellar gene transcriptional hierarchy is composed of four classes of flagellar genes. Class I is only composed of *flrA*, which encodes an RpoN-dependent activator. FlrA together with RpoN is required for the expression of class II genes that encode components of the MS ring-switch and for the regulatory proteins FlrB, FlrC and FlrA (σ^{28}). Class III genes are dependent on FlrC and RpoN for their expression and encode the basal body, hook and core

Table 1. Phenotypes of phase variants and the regulatory mutants.

Strain	Colony morphology ^a	Pellicle formation ^b	Hydrophobicity ^c	Motility ^d
Smooth	Flat, smooth	–	3	100
Rugose	Raised, very corrugated	+++	8	46.3
<i>ShapR</i>	Raised, corrugated	++	6	60
<i>RhapR</i>	Raised, super corrugated	++++	10	18.2
<i>SrpoS</i>	Raised, smooth	+	ND	ND
<i>RvpsR</i>	Flat, smooth	–	3	48.7
<i>SvpsR</i>	Flat, smooth	–	ND	ND
<i>RrpoN</i>	Flat/raised, wrinkled	++	ND	12
<i>SrpoN</i>	Flat, smooth	–	ND	10

a. Colonial morphologies developed after 48 h of incubation on LB agar plates at 30°C.

b. Pellicles developed at the air–water interface in a 15 ml test tube filled with 5 ml of LB and incubated under static conditions at 30°C for 48 h.

c. Hydrophobicity as determined by the direction of spreading method on a bacterial lawn developed after 48 h growth on LB plates at 30°C. For this technique, bacterial lawns are grown on an agar surface. Then, a drop of water is placed at the border between the bacterial lawn and an agar, glass or polystyrene surface. The behaviour of the water drop at these borders provides a measure of relative hydrophobicity because water moves away from the most hydrophobic surface. The most hydrophobic of the assayed bacteria is arbitrarily assigned a score of 10, whereas the most hydrophilic of the assayed bacteria is assigned a score of 1.

d. Motility detected using 0.3% LB agar plates after 24 h of incubation at 30°C. Numbers are expressed as a percentage relative to the smooth variant.

flagellin (FlaA), flagellar cap (FliD) and motor component (MotX). Class IV genes are dependent on alternative sigma factor σ^{28} and encode an alternative flagellin and motor components. Expression of some of the class III and IV genes was significantly lower in the rugose phase variant compared with the smooth variant. In contrast, expression of the class I and class II genes was not significantly different in the two phase variants. In view of the effect of colony morphotype on the expression of some flagellar biosynthesis genes, we used soft agar

plates to determine motility zones exhibited by the wild-type rugose and the smooth phase variants. The motility diameter of the rugose phase variant after 24 h of incubation at 30°C on LB soft agar motility plates was 46% compared with the smooth variant (Fig. 3A). However, when analysed by phase-contrast microscopy, the swimming behaviour of the rugose phase variant was qualitatively similar to that of the smooth phase variant, and transmission electron microscopy (TEM) studies showed that the rugose variant synthesizes and retains flagella of

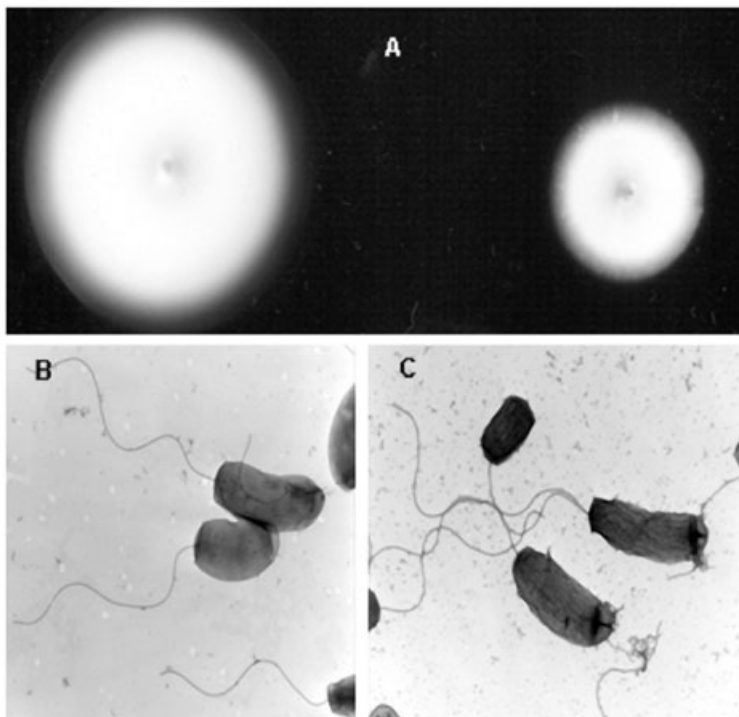


Fig. 3. Motility and flagellation of phase variants. Zone of motility for the smooth (A, left) and rugose (A, right) variants grown on 0.3% LB agar plates at 30°C for 24 h. Presence of flagella was analysed by electron microscopy using negatively stained smooth (B) and rugose (C) variants.

normal length and structure (Fig. 3B). Thus, at present, it is unclear what the significance of decreased flagellar gene transcription is for the formation of rugose colonies. In *V. cholerae* O139, mutation of *flaA* (flagellin A) leads to rugose colonial morphology (Watnick *et al.*, 2001). This result and our observation that *flaA* expression is repressed in the rugose variant indicate that, in *V. cholerae*, there is an inverse correlation between the expression of VPS genes and the expression of the class III and class IV flagellum biosynthesis genes. The nature of this regulation has yet to be determined.

Motility and chemotaxis are often co-regulated functions. The *V. cholerae* genome sequencing project identified 43 methyl-accepting chemotaxis proteins (Heidelberg *et al.*, 2000). Of these, the expression of four (VC2213, VCA0864, VCA0923, VCA1069) was induced and one (VC1413) was repressed in the rugose compared with the smooth variant during exponential phase growth in a liquid medium. In addition, the expression of four genes (VC1399, VC1401, VC1402, VC1403) in a cluster of chemotaxis genes (VC1397–VC1404) was repressed in the colonies of the rugose phase variant (data not shown). *V. cholerae* has multiple homologues of *Escherichia coli* chemotaxis genes, and these are clustered into three different regions (Heidelberg *et al.*, 2000). However, in contrast to *E. coli*, little is known about *V. cholerae* chemotaxis. It has been shown recently that only one of the three *cheA* homologues (*cheA-2*) is responsible for chemotaxis in the Classical and El Tor *V. cholerae* O1 biotypes when assayed in 0.3% LB soft agar motility plates (Gosink *et al.*, 2002). These results and those obtained here suggest that the chemotactic behaviours of the smooth and rugose phase variants of *V. cholerae* are likely to be different. Consequently, the reduced motility behaviour of the rugose variant could result from a combination of effects: a reduction in the expression of certain flagellar biosynthesis genes and differences in chemotaxis functions. From an evolutionary perspective, switching between the rugose and smooth colony morphotypes may contribute to the survival of the organism in different environments owing, in part, to its effect on motility and chemotaxis and thus on the distribution of *V. cholerae* within an ecosystem.

Comparison of the smooth and rugose phase variant expression profiles led to the identification of 12 differentially expressed genes that are predicted to encode proteins with regulatory functions (Heidelberg *et al.*, 2000). Included in this group are 11 genes that are induced in the rugose variant: VC0486 (DeoR family transcriptional regulator), VC0665 (*vpsR*), VC0706 (sigma 54 modulation protein, putative), VC0791 (sensor kinase, *citA*), VC1076 (transcriptional regulator, AraC/XylS family), VC1081 (response regulator), VC1349 (sensory box sensor histidine kinase/response regulator), VCA0238 (sen-

sor histidine kinase), VCA0239 (response regulator), VCA0917 (transcriptional regulator, TetR family) and VCA0952 (transcriptional regulator, *luxR* family). We reported previously that expression of the *vpsR* gene was similar between the smooth and rugose variants (Yildiz *et al.*, 2001). Here, we find it to be induced in the rugose compared with the smooth variant. We believe that this discrepancy results from differences in the growth state of the samples used for these comparisons. One gene coding for a putative transcription factor, VCA0697 (sensory box/GGDEF family protein), was repressed in the rugose variant. The role of these regulatory factors in maintaining the colony morphotypes is under investigation.

Expression of the sulphur assimilation gene VC0386 (*cysH*) and VC1061 (encoding for cysteine synthase) was low in the rugose wild-type variant compared with the smooth variant. In *E. coli*, the expression of *cys* regulon genes is induced by sulphur limitation and is dependent on the transcriptional regulator CysB and inducer *N*-acetylserine (Kredich, 1996). End-product cysteine leads to feedback inhibition of serine acetyltransferase, which catalyses the formation of O-acetylserine from which inducer *N*-acetylserine is derived (Kredich, 1996). Examination of the *V. cholerae* O1 El Tor N16961 genome sequence revealed the presence of three genes encoding for serine acetyltransferase (Heidelberg *et al.*, 2000). Two of them, VC0919 and VC0923, are located in the *vpsI* cluster, and their expression is increased in the rugose variant relative to the smooth variant. The third gene, VC2649, located elsewhere in the large chromosome, is not differentially regulated. It is likely that increased expression of serine acetyltransferase in the rugose variant may lead to increased production of L-cysteine, which may in turn cause feedback inhibition of the *cys* regulon. Thus, depending on the balance of cysteine biosynthesis and use, the cysteine pool in the rugose variant may be lower than that in the smooth variant. If so, this could lead to a decrease in the production of homocysteine and in turn reduction in the amount of *S*-adenosyl-L-methionine (SAM) synthesized. It is of interest that both quorum-sensing autoinducers (AI-1 and AI-2) are derived from SAM (Schauder *et al.*, 2001). Thus, differences in metabolic pathways that affect the production of SAM may alter the production of quorum-sensing molecules in the rugose strain compared with the smooth strain. Based on the above argument, autoinducer production in the rugose variant is expected to be lower/delayed relative to that in the smooth variant. Inability to produce 'normal' levels of AI would mimic a low cell density condition in which LuxO has been shown to repress transcription of *hapR* (Zhu *et al.*, 2002). Indeed, *hapR* message levels in the rugose variant were found to be minimally, but consistently, reduced.

The identification of rugose phase variation-expressed genes that are regulated by the presence of VPS^{EITor} or by its production or secretion

The rugose phase variant expresses *vpsI* and *vpsII* genes coding for polysaccharide biosynthetic functions and produces an abundant extracellular matrix containing VPS^{EITor} (Yildiz and Schoolnik, 1999). In turn, this extracellular material increases the tendency of rugose phase variant cells to autoaggregate, exhibit chlorine resistance and form hydrophobic, corrugated colonies and high-profile biofilms (Yildiz and Schoolnik, 1999). Microarray expression experiments were conducted to identify genes in the rugose phase variant expression profile with differential regulation that is not the result of phase variation *per se*, but rather comes from the presence of VPS^{EITor} on the cell surface or from its production and/or exportation. The expression profile of the wild-type rugose phase variant was compared with the expression profile of a *vpsA* mutant in the rugose genetic background under the same conditions of growth. The *RvpsA* mutant lacks all the typical properties of the rugose phase variant: it exhibits a smooth colonial morphotype, forms a low-profile biofilm and does not autoaggregate (Yildiz and Schoolnik, 1999).

Comparison of whole-genome expression profiles of the rugose and *RvpsA* strains during exponential phase growth revealed that 39 genes were induced and 20 genes were repressed in *RvpsA* relative to the rugose variant (a complete list is provided in *Supplementary material*, Appendix S2). *RvpsA* harbours a transposon insertion into *vpsA* and because of polarity effects prevents transcription of *vpsI* operon genes. As expected, expression of 11 genes located in the *vpsI* operon was repressed in the *RvpsA* mutant.

Genes required for the transport of carbohydrates, amino acids and peptides as well as energy metabolism genes (TCA cycle, pentose phosphate pathway, glycolysis and gluconeogenesis) were induced in the *vpsA* mutant relative to the rugose variant. It is likely that the production of VPS^{EITor}, the major sugars of which are glucose and galactose, requires *de novo* glucose synthesis when grown in LB where amino acids provide most of the carbon and energy. Thus, disruption of VPS^{EITor} synthesis in *RvpsA* appears to affect carbon flux and metabolism.

Comparison of the transcriptomes of the smooth and rugose phase variants identified 124 genes (S/R *pvr* genes) that were differentially regulated between the phase variants. To discover which of the S/R *pvr* genes are not regulated by the presence of the VPS matrix, the transcriptomes of the smooth variant and *RvpsA* mutant were compared. This comparison revealed that, during exponential phase growth, 76 of the 124 S/R *pvr* genes, including *vps* region genes, *eps* genes, flagellar genes

and a set of regulatory genes (VC0665 VC1076, VC1081, VCA0952, VCA0697), continue to be differentially regulated in a phase variation-dependent manner (*Supplementary material*, Appendix S3). Thus, the expression of these genes does not depend on the presence of the VPS^{EITor} matrix. Together, these results show that, although VPS^{EITor} on the cell surface influences gene expression, it does not control the expression of most S/R *pvr* genes.

Identification of the HapR regulon by microarray expression profiling

The transcriptional regulator HapR is a member of the quorum-sensing circuit in *V. cholerae*, recently shown to regulate virulence and biofilm development phenotypes negatively (Zhu *et al.*, 2002; Hammer and Bassler, 2003; Zhu and Mekalanos, 2003). We identified negative regulator(s) of rugose colonial morphology by screening a Tn5 transposon library, prepared in the smooth variant genetic background, for pellicle-forming mutants. Analysis of a set of these mutants showed that they had sustained insertions into *hapR*, an event that caused conversion of the smooth colony morphotype to the corrugated and opaque colonial morphology of the rugose phase variant, thus independently confirming a previous observation by Jobling and Holmes (1997). We generated a *hapR* null mutant in both smooth and rugose genetic backgrounds by insertional mutagenesis. Like the transposon mutant, the *hapR::pGP704* mutant in the smooth genetic background, henceforth denoted *ShapR*, formed colonies with the rugose morphotype. When *hapR* was mutated in the rugose genetic background, denoted *RhapR*, corrugation of the colonial surface and cell surface hydrophobicity – normal properties of wild-type rugose colonies – were enhanced. Thus, loss of *hapR* converts smooth into rugose, whereas loss of *hapR* in the rugose background produces a super rugose morphotype. As we observed a phenotype (i.e. the super rugose morphotype) when *hapR* was disrupted in the rugose genetic background, we surmised that the original wild-type rugose phase variant did not result from a mutation of the *hapR* gene. We were able to complement these mutants by introducing an intact copy of the *hapR* gene from the wild-type smooth strain. These findings strongly suggest that *hapR* is not the site of the smooth-to-rugose phase variation event in the EITor strain used here.

To identify genes whose regulation that is HapR dependent, we compared the gene expression pattern of the *ShapR* mutant with the wild-type smooth colonial variant during exponential growth. Analysis of these microarray expression profiles identified 111 and 54 genes, respectively, which were negatively and positively regulated by HapR in the smooth genetic background (a complete list

is provided in *Supplementary material*, Appendix S4). Hierarchical cluster analysis (Eisen *et al.*, 1998) of these expression profiles was performed to identify and group functionally, according to their expression patterns, subsets of the 124 S/R *pvr* genes that are HapR dependent (Fig. 1A). The expression of genes in the *vpsI* and *vpsII* clusters was found to be induced in the *ShapR* mutant compared with the smooth strain (Fig. 1A–C). Similarly, increased *eps* gene expression was observed in the *ShapR* mutant (Fig. 1A and B). Taken together, these results show that HapR represses functions required for the production and secretion of VPS^{EITor} in the smooth colonial variant. Five genes predicted to encode transcription factors were also induced in *ShapR* (VC0486, VC0665, VC0706, VC1081, VCA0952); among these is VC0665, which encodes VpsR, a previously described positive regulator of *vps* gene expression (Yildiz *et al.*, 2001). In contrast, Hammer and Bassler (2003) reported that *vpsR* transcription was not controlled by the quorum-sensing circuit in *V. cholerae* O1 El Tor strain C6706. This discrepancy may result from differences in the strains used. In our A1552 prototype strain, the above-described expression profiling results are consistent with the idea that HapR negatively regulates *vps* gene expression in the smooth genetic background indirectly, by repressing *vpsR* expression, or directly, by repressing *vpsI* and *vpsII*. It is also possible that HapR acts at both sites – repressing both *vps* and *vpsR* expression. In contrast, expression of a set of flagellar genes (VC2141, VC2142, VC2143, VC2187, VC2188, VC2190, VC2191, VC2196, VC2197) is repressed in *ShapR*, indicating that HapR is required for their transcription. Thus, HapR appears to exert opposite effects on VPS^{EITor} production and motility. Promoter motif analysis revealed the presence of the HapR binding site upstream of the flagellar genes (*Supplementary material*, Appendix S11), suggesting that its effect on the latter function is direct.

Because HapR-dependent changes in motility and VPS^{EITor} production could affect biofilm development, quantitative differences in the biofilms formed by the *ShapR* mutant and smooth variant of the wild-type parent were measured by monitoring the intensity of crystal violet staining of biofilms on the surface of a microtitre well as a function of time. After 6 h of biofilm development, the biofilm-forming capacity of the *ShapR* mutant was 7.5-fold greater than that of the smooth variant of the parent strain (Fig. 2A). However, the biofilm-forming capacity of *ShapR* was still 1.5-fold less than that of the wild-type rugose variant, indicating that other regulators of *vps* gene expression, in addition to *hapR*, might suppress VPS^{EITor} production in the smooth variant. Alternatively, this result might also indicate that the full expression of the biofilm phenotype by the wild-type rugose variant requires HapR-independent genes that are expressed in the rugose

genetic background. Unexpectedly, the biofilm-forming capacity of the *RhapR* mutant was also lower than that of the rugose variant (Fig. 2A). However, inspection of the microtitre wells showed that this may have been caused by the increased pellicle-forming capacity of the *RhapR* mutant and the accumulation of biomass at the air–liquid interface, thus decreasing the number of *RhapR* bacteria available for adherence to the plastic surface. As pellicles are a kind of biofilm, the biofilm-forming capacity of pellicle-forming bacteria, such as the *RhapR* mutant, is not accurately represented by the crystal violet staining assay. The biofilm phenotypes of *ShapR* and *RhapR* were complemented by introducing PACYC184 containing a wild-type copy and upstream regulatory region of *hapR* (data not shown).

To determine the structure of biofilms of the rugose and smooth *hapR* mutants, biofilms were formed under flow conditions and analysed by CSLM. The structure of *ShapR* biofilms was morphologically more like the rugose than the smooth variant (Fig. 2B). Intriguingly, the biofilm morphology of the *RhapR* mutant did not exhibit pillar-like structures and was more compact and less developed with an average thickness of only 17 µm. Concurrent with this observation, the roughness of *RhapR* biofilms was found to be less than that of the rugose variant. In addition, the surface to biovolume ratio, which is a measure of biofilm porosity (compact biofilms will have low surface to volume ratios), was lower than that of rugose and *ShapR* biofilms. Thus, results from both static and flow biofilm assays show dramatic differences in the development and structure of *RhapR* and *ShapR* biofilms.

As the transcriptome analysis of the *ShapR* mutant and smooth variant indicated that flagellar gene transcription is positively regulated by HapR, we compared the motility of the *hapR* mutants with their corresponding wild-type parents. Using the soft agar motility assay, the swarm diameter size of the *ShapR* mutant was found to be only 60% of the wild-type smooth variant. Most strikingly, the *RhapR* mutant exhibited a dramatic reduction in swarm size (18% of the smooth variant and 39% of the rugose variant from which it was derived), a defect that is quantitatively similar to the *rpoN* mutant that does not synthesize flagellum (Table 1). When analysed by electron microscopy, we observed that the majority of the *RhapR* cells did not produce flagella. Therefore, differences between the motility behaviours and cell surface properties (specifically cell surface hydrophobicity; Table 1) of the *RhapR* mutant and its rugose wild-type parent are likely to be responsible for the observed differences in their biofilm phenotypes.

Including the *fla* and *vpsI/vpsII* genes described above, the expression of 37 genes was found to be HapR dependent in both smooth and rugose genetic backgrounds. Thus, the regulation of this gene set by HapR is colony

phase variation independent. Here, we discuss a subset of these genes. The expression of five genes located in a cluster on the large chromosome [VC0199 (haemolysin secretion ATP-binding protein), VC0200 (iron III compound receptor), VC0201 (iron III ABC transporter, ATP-binding protein), VC0202 (iron III ABC transporter, periplasmic iron compound-binding protein), VC0203 (iron III ABC transporter, permease protein)] (Heidelberg *et al.*, 2000) was increased in the *ShapR* and *RhapR* mutants compared with their expression in the wild-type smooth colonial variant. Similarly, the expression of VCA0219 (*hylA*, haemolysin) was increased in the *ShapR* and *RhapR* mutants. Thus, functions required for iron acquisition, and specifically for iron III transport, are repressed by HapR. However, this effect may be secondary to increased VPS^{EITor} production by these *hapR* mutants, as this polysaccharide appears to deplete iron from the media as determined by expression profiling studies of the smooth colonial variant incubated with purified VPS^{EITor}, which showed induction of iron-scavenging pathways (N. A. Dolganov, personal communication).

VC1034 (uridine phosphorylase, *udp-1*), VC2348 (phosphopentomutase, *deoB*), VC2349 (thymidine phosphorylase, *deoA*) and VCA0053 (purine nucleoside phosphorylase, *deoD-2*) were more strongly expressed in the *ShapR* mutant compared with the wild-type smooth colonial variant, indicating that these genes are normally repressed by HapR. The products of these genes are involved in the catabolism of nucleotides for use as an energy and carbon source as well as for the synthesis of nucleotides (Zalkin, 1996). Expression of these genes is under the control of the CytR repressor, DeoR repressor and cAMP–CRP complex in *E. coli* (Zalkin, 1996). Interestingly, it was shown recently that a *cytR* mutation in *V. cholerae* O139 leads to increased expression of *udp-1* (VC1034) (Haugo and Watnick, 2002). Furthermore, the *cytR* mutant displayed a rugose colonial morphology and exhibited increased *vpsL* expression compared with the wild-type parent (Haugo and Watnick, 2002). This finding showed that CytR is acting as a repressor of exopolysaccharide biosynthesis and, in turn, biofilm formation. As the CytR mutant exhibits an increased capacity to take up nucleosides, it was suggested that an increase in intracellular cytidine levels is used as a signal for switching to the biofilm growth mode from the planktonic one (Haugo and Watnick, 2002). Alternatively, increased nucleoside levels in the cell may lead to an increase in the formation of activated sugar nucleotide intermediates, which would in turn increase exopolysaccharide synthesis. As a result, the increased production of exopolysaccharide could lead to an increased capacity to attach to surfaces and form biofilm matrix material. These results with *V. cholerae* O139 are congruent with our microarray expression results with *V. cholerae* O1 El Tor, which show

that the *vpsI* and *vpsII* genes and *udp-1* are negatively regulated by HapR.

HapR is part of the quorum-sensing system of *V. cholerae*, and its expression is repressed by the action of LuxO (Zhu *et al.*, 2002). LuxO is an *RpoN*-dependent response regulator, its activity is controlled by the phosphorylation state of the protein and, when LuxO is phosphorylated at low cell density, it prevents *hapR* transcription (Klose *et al.*, 1998; Zhu *et al.*, 2002). In contrast, at high cell density, LuxO is dephosphorylated, expression of *hapR* is increased, and HapR downregulates the expression of pathogenesis genes through its action on *aphA* (Kovacikova and Skorupski, 2002a). Our results also confirmed this finding as transcription of *aphA* was found to be increased by 1.78-fold in the *ShapR* mutant relative to the wild-type parent (data not shown). However, under the low cell density experimental condition used in this study (OD₆₀₀ of 0.3–0.4 in LB broth), when *hapR* is expected to be silent owing to repression by phosphorylated LuxO, the expression of *ctxAB* operon genes (encoding cholera toxin) and *tcp* genes (encoding proteins required for the biogenesis of the toxin co-regulated pilus) was the same for the *ShapR* mutant and the wild-type smooth parent. However, when we compared the gene expression profiles of bacteria obtained from wild-type smooth and *ShapR* mutant colonies, grown for 24 h on LB agar – a high cell density condition of growth – the expression of the *ctx* and *tcp* genes was dramatically upregulated in the *ShapR* mutant (data not shown).

The results described above did not identify which of the HapR-dependent genes are directly regulated by HapR, i.e. by interaction of this transcription factor with the corresponding promoters. The HapR promoter-binding motif in *V. cholerae* was defined empirically by Kovacikova and Skorupski (2002a) through the use of gel shift and DNase I footprint assays of the upstream regulatory region of *aphA*. We used the empirically defined HapR-binding motif to survey the promoters of the HapR-regulated genes that had been identified in this study by expression profiling experiments. We scanned the promoters of all the genes to find 14-mers that matched well with the TGAGAWWWTCTCA palindrome motif, with increased weight at the second base 'G' and second to last base 'C' in the consensus, as they were shown to be critical for HapR binding (Kovacikova and Skorupski, 2002a). We identified this motif in the upstream region of 269 genes (a complete list is provided in *Supplementary material*, Appendix S11); 57 of these showed differential expression (fold change ≥ 1.3 or ≤ 0.8) in the smooth versus *ShapR* gene expression profiling experiment. Our analysis identified the consensus sequence in the promoter region of VC2647 encoding for AphA and in the upstream regulatory region of the *vpsI* operon (VC0917–VC0927), which contains genes with average expression

that was 3.99-fold higher in the *ShapR* mutant. The upstream regions of several genes encoding for regulatory functions were also found to have the HapR-binding motif, including VC0486 and VC1076, which are expressed at a higher level in the rugose wild-type phase variant and *ShapR* mutant compared with the smooth variant. We also identified the motif in the promoters of VC1034 and VC2677 encoding for uridine phosphorylase and CytR respectively. The presence of the HapR motif in both *cytR* and *vpsI* promoters suggests that HapR negatively regulates *vpsI* expression at two or more levels: by increasing the expression of *cytR* (a negative regulator of *vpsI* expression) and by directly binding and reducing the activity of the *vpsI* promoter. The promoter regions of some genes required for chemotaxis and motility functions were also found to contain the HapR binding site. Finally, the HapR binding site motif was found in the promoter regions of genes with diverse cellular roles indicating its global importance for cell function.

We also subjected the whole-genome expression profiling results discussed above to the sequence motif finding algorithms MOTIF REGRESSOR (Conlon *et al.*, 2003) and BIOPROSECTOR (Liu *et al.*, 2001) to identify possible motifs in the upstream non-coding sequences of the differentially regulated genes. The most significant motif identified by these algorithms in the smooth versus *ShapR* gene expression profiling data set was a long (≈ 100 bp) conserved motif in the promoter region of 99 open reading frames (*Supplementary material*, Appendix S10). All appeared to be on the same strand in a relatively short region spanning 119 transcripts on the small chromosome. Using an entirely different approach, this motif was also found by Mazel *et al.* (1998) and Rowe-Magnus *et al.* (2001) and designated a *V. cholerae* repeat sequence (VCR); whole-genome sequencing confirmed the presence of a large integron island (a gene capture system) in this region (Heidelberg *et al.*, 2000). Most of the 99 genes are annotated by TIGR as encoding for hypothetical proteins. The microarray expression results reported in this study showed that these genes are not only transcribed, but also exhibit strong differential expression in the *hapR*, *rpoS* and *rpoN* mutants. The expression of 94 of the 99 genes in this island was downregulated in the *ShapR* mutant compared with the wild-type smooth variant, with an average fold change of 0.74. Expression of 84 of them was also downregulated in *SrpoS* relative to wild type with an average expression fold change of 0.66. Furthermore, we observed that the expression of 82 of these genes was increased in the *rpoN* mutant compared with the wild-type rugose strain with an average expression fold change of 1.68. Thus, our results suggest that many genes in the integron island are positively regulated by HapR and RpoS and negatively regulated by RpoN. HapR is induced at high cell densities and RpoS in

response to stress and during stationary phase growth. Consequently, integron island genes might be expected to be activated in crowded, stressed communities containing non-replicating organisms. When viewed from an environmental and evolutionary survival perspective, this behaviour could confer a survival advantage because it would integrate a gene acquisition programme (enhancing genetic diversity, plasticity and versatility) with a survival-enhancing stress response.

The effect of RpoS on HapR-dependent gene expression

RpoS facilitates adaptation of bacteria to stress and controls the expression of many genes during both exponential and stationary phases of growth (Hengge-Aronis, 1993; 2002a,b). We showed previously that *rpoS* is also required for the production of HA/P by *V. cholerae* O1 El Tor (Yildiz and Schoolnik, 1998). As the expression of *hap* is positively regulated by HapR, the involvement of RpoS in the regulation of *hapR* was examined using expression profiling to compare transcripts of an *rpoS* mutant in the smooth genetic background (designated *-SrpoS*) with transcripts from the wild-type smooth colonial variant during exponential phase growth in LB broth. Fifty-two genes were found to be induced and 119 genes repressed in *SrpoS* compared with the smooth colonial variant; a complete list of these genes is provided in *Supplementary material*, Appendix S5. Expression of VC0583, encoding *hapR*, was reduced 3.3-fold in the *SrpoS* mutant, indicating that *rpoS* is required for transcription of *hapR* during exponential phase growth. Intriguingly, expression of *hap* (VCA0865) was not altered during exponential growth in either *ShapR* or *SrpoS*. In contrast, when analysed on colonies formed after 24 h of incubation on LB plates, *hap* expression was reduced by 8.48-fold in *ShapR* and 3.48-fold in the *SrpoS* mutant compared with the wild-type smooth colonial variant. The results indicate that expression of *hap* is regulated by the combined effects of HapR and RpoS and is growth phase and/or cell density dependent. Similarly, in wild-type smooth and *SrpoS* mutant colonies, grown for 24 h on LB agar, the expression of the *ctx* and *tcp* genes was dramatically upregulated in the *SrpoS* mutant (data not shown).

To discriminate between the effects of RpoS and HapR on gene regulation, microarray expression profiles of the *SrpoS* mutant and the *ShapR* mutant were compared with the wild-type smooth phase variant. The results showed that expression of only a small set of genes (24 induced/23 repressed) was similarly regulated between the two mutants. Genes predicted to be functioning in iron III transport (VC0199–VC0203) were upregulated in both mutants to the same degree. In addition, expression of *vpsII* operon genes was induced relative to the smooth wild-type variant in both *ShapR* and *SrpoS* mutants and,

like *hap* gene expression, the magnitude of induction of *vpsII* operon genes was greater for the *hapR* mutant than for the *rpoS* mutant. Interestingly, expression of VCA0952 (encoding for a transcriptional regulator) was also higher in the *ShapR* mutant relative to *SrpoS*. We have mutated VCA0952 (now designated *vpsT*) in the rugose variant and showed that it is required for the development of rugose colonial morphology. We also showed that the expression of the *vps* genes, *vpsR* and *vpsT*, is positively regulated by the VpsT transcriptional regulator (Casper-Lindley and Yildiz, 2004).

The well-established relationship between VPS^{E₁} production and biofilm formation led us to compare the biofilm-forming capacities of the *SrpoS* mutant and the wild-type smooth variant. As predicted from the effect of RpoS as a positive regulator of *hapR* expression (which in turn negatively regulates *vps* expression), the biofilm-forming capacity of the *SrpoS* mutant was found to be 3.6-fold greater than that of the wild-type smooth variant (Fig. 2A). When the biofilm morphology of the *SrpoS* mutant, formed under flow conditions, was compared with that of the smooth parent, we observed that the biofilm structures of the two strains were similar, but not identical (Fig. 2B). The *SrpoS* mutant clearly produced more matrix material, was thicker and had a lower surface to biovolume ratio than the smooth biofilm. In contrast, the *SrpoS* mutant biofilm was less developed relative to the *ShapR* mutant. As the capacity to produce exopolysaccharide modulates characteristics of colonial morphology, we compared the colonial morphologies of the *SrpoS* mutant with the smooth wild-type variant. The *SrpoS* mutant forms smooth colonies. However, the colonies are more compact and raised compared with the flat colonies of the wild-type smooth parent, indicating that *rpoS* probably modulates VPS^{E₁} accumulation and may thus be required for the flat colonial morphology of the wild-type smooth variant.

The expression of a large set of HapR-regulated genes (109) was not affected by the *rpoS* mutation. Consequently, the regulation of *hapR* transcription by RpoS cannot account for many of the differentially expressed genes observed in the *hapR* mutant.

Identification of the VpsR regulon

Disruption of *vpsR* in the rugose genetic background (denoted *RvpsR*) reduces *vps* gene expression and yields phenotypically smooth colonies. Under static conditions, the *RvpsR* mutant forms a low-profile biofilm that resembles biofilms formed by the wild-type smooth colonial variant (Yildiz *et al.*, 2001). To identify genes with regulation that is VpsR dependent in the rugose genetic background, we compared whole-genome expression profiles of *RvpsR* with profiles of the wild-type rugose parent during exponential phase growth. The expression of 118 genes

by the *RvpsR* mutant was lower compared with their expression by the wild-type rugose variant, indicating that they require VpsR for their expression in the rugose genetic background (a complete list is provided in *Supplementary material*, Appendix S6). Among these are *vps* genes, which encode VPS^{E₁} biosynthetic enzymes (Fig. 4B), thus corroborating previous real time polymerase chain reaction (PCR) results; and *eps* genes (Fig. 4C), which encode components of the type II secretion system that is postulated to be required for the export/secretion of VPS^{E₁}. Expression of regulatory genes VC0706, VC1076, VC1081, VC1349, VCA0238, VCA0239, VCA0917 and VCA0952 was also found to require VpsR in the rugose variant. It is not clear whether VpsR directly regulates expression of these genes. Unfortunately, a large set of the VpsR upregulated genes (44 out of 118) encode for hypothetical/conserved hypothetical proteins or proteins of unknown functions (14 out of 118). Thus, the functions of $\approx 50\%$ of the genes that are positively regulated by VpsR are unknown. Consequently, other than genes required for VPS production and secretion, a general functional theme for the VpsR regulon was not identified.

The expression of 173 genes was higher in the *RvpsR* mutant compared with the wild-type rugose parent, indicating that their expression is normally repressed through the action of VpsR. Expression of a large set of genes required for energy metabolism and nutrient transport was increased in the *RvpsR* mutant. It is unlikely that all these genes were repressed directly by VpsR as expression of a number of transcriptional factors is regulated by VpsR.

Transcriptome analysis revealed that some of the nucleoside uptake and catabolism functions are repressed by VpsR as expression of *nrdA* (VC1256), encoding the alpha subunit of ribonucleoside diphosphate reductase, *udp-1* (VC1034), *deoB* (VC2348) and *nupC* family protein (VC2352), is increased in the *RvpsR* mutant relative to the rugose variant. Interactions between nucleoside salvage pathways and carbon metabolism are complex and are adjusted according to the needs of the organism. Results from our studies suggest that VpsR, directly or indirectly, plays a central role in making these adjustments.

Expression of *aphA* (VC2647) encoding for a regulatory protein that positively activates *tcpPH* transcription was decreased in the *RvpsR* mutant relative to the wild-type rugose variant, suggesting that transcription of *aphA* is positively regulated by VpsR. The expression of *aphA* was also consistently lower in the *SvpsR* mutant than in the wild-type smooth variant (data not shown). However, under the experimental conditions used (i.e. during exponential growth in LB broth), we did not observe a significant change in the expression of the major virulence genes. It is important to note that *aphA* message abundance was

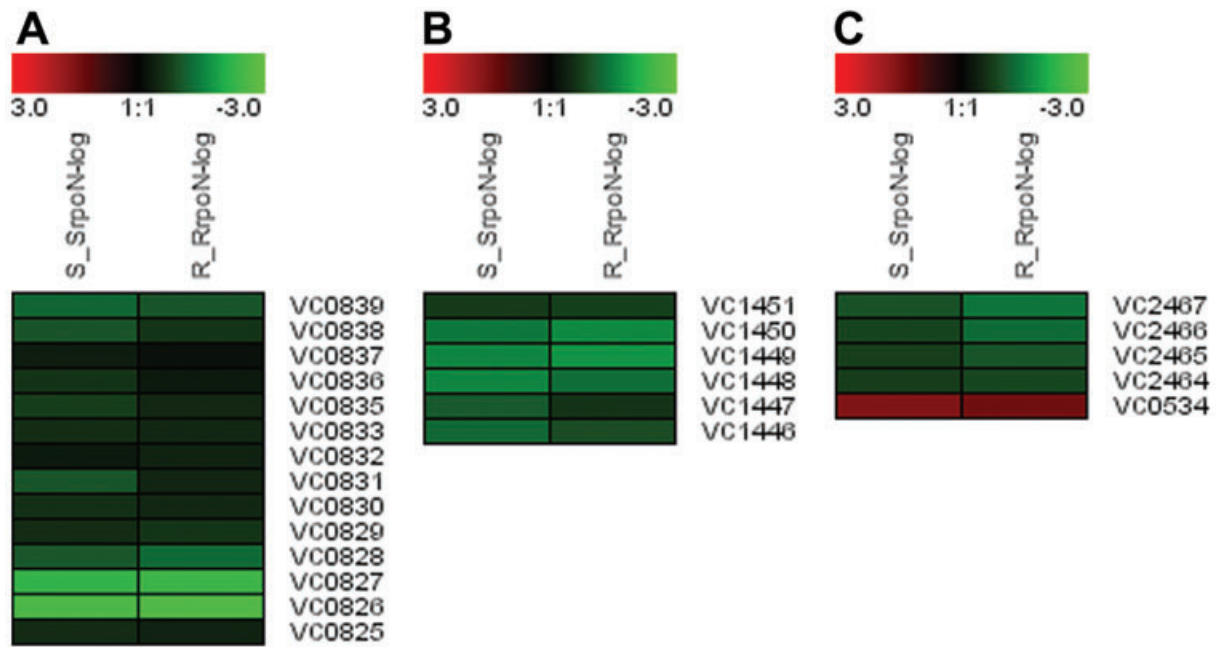


Fig. 4. Display of set of *rpoN*-regulated genes in genome order. Expression profiles of the *tcp* gene cluster (A), *rtx* genes (B) and sigma factors (C) in the *SrpoN* and *RrpoN* mutants relative to wild-type parents. Expression ratios are depicted according to the colour scale shown at the top. Each column represents an experiment; the gene expression profiles are represented in rows.

increased approximately twofold in the *SrpoS* mutant and decreased more than twofold in the *RrpoN* and *SrpoN* mutants, indicating that *aphA* is likely to be the major control point in the regulation of the virulence cascade.

To elucidate the role of *vpsR* in the smooth variant, we mutated *vpsR* in the smooth genetic background (denoted *SvpsR*) and compared gene expression profiles of *SvpsR* with the smooth variant using total RNA isolated from exponentially grown cells. The results revealed that 64 genes (24 induced and 40 repressed) are regulated by *VpsR* in the smooth variant (a complete list is provided in *Supplementary material*, Appendix S7); 48 of these were similarly regulated in *SvpsR* and *RvpsR*. For example, genes located in the *vps* region, VC1888 (haemolysin-related protein), VCA0864 (methyl-accepting chemotaxis protein) and transcriptional regulator VCA0952 were positively regulated by *VpsR*. In contrast, genes involved in nucleoside catabolism (VC1255, VC1256, VC1034, VC2348) were negatively regulated by *VpsR* in both genetic backgrounds. Thus, the *VpsR* regulons of the rugose and smooth variants share common and unique sets of genes.

Empirically determined promoter motifs of *VpsR*-regulated genes have not been reported. Therefore, we analysed the expression profiling results discussed above with the sequence motif finding algorithms MOTIF REGRESSOR (Conlon *et al.*, 2003) and BIOPROSPEROR (Liu *et al.*, 2001) to identify possible *VpsR*-binding motifs in the upstream non-coding sequences of the differentially regulated

genes. MOTIF REGRESSOR identified a highly significant palindrome motif (P -value $< 10E-16$) for smooth versus rugose and rugose versus *RvpsR* differentially regulated genes. This motif has a relatively degenerate AT-rich pattern in the middle and a more conserved core half-site TCTCA at the two ends. We used this computationally determined *VpsR*-binding motif to screen all the promoter sequences of the genome to identify the 190 genes with upstream promoter regions that have sequences that best match this motif (a complete list is provided in *Supplementary material*, Appendix S12). Expression of 25 of these genes was found to be reduced by a fold change ≥ 0.7 in the rugose versus *RvpsR* transcriptome analysis. Interestingly, VC0930, VC0929 and VCA0075 not only contained some of the highest scoring sites, but also harboured three, two and two copies of this motif respectively. Therefore, we hypothesize that this motif is recognized directly by *VpsR* or by one of the regulatory proteins controlled by *VpsR* to regulate transcription in *V. cholerae*. In contrast, VC0917 (*vpsA*), the first gene in the *vpsI* operon, did not contain this motif and thus might not interact directly with *VpsR*.

The identification of RpoN regulons and HapR- and VpsR-regulated genes that require RpoN

VpsR, a positive regulator of *vps* gene expression, belongs to the NtrC subclass of response regulators that acts in concert with alternative sigma factor RpoN (North

et al., 1996). If VpsR and RpoN interact in this way, then the phase variation-associated genes, including *vps* polysaccharide biosynthetic and *eps* type II secretion genes, might require both VpsR and RpoN for their expression. In addition, the expression of *hapR*, a negative regulator of *vps* gene expression in the smooth genetic background, is reduced at low cell densities by the quorum-sensing transcription factor LuxO (Zhu *et al.*, 2002). Like VpsR, LuxO also requires RpoN to regulate gene expression (Klose *et al.*, 1998). Thus, RpoN, via its effect on LuxO, is predicted to induce *vps* gene expression by downregulating the expression of HapR. Therefore, whether it affects *vps* gene expression via its action on LuxO or on VpsR or both, deletion of *rpoN* is predicted to reduce *vps* gene expression. To test this prediction and to appreciate better the global effect of RpoN on gene regulation, *rpoN* mutants in the rugose and smooth genetic backgrounds (designated *RrpoN* and *SrpoN* respectively) were compared with the corresponding wild-type phase variant by microarray expression profiling during mid-exponential phase growth in LB broth. It should be noted that the growth rates of the *rpoN* mutants were not altered when compared with each other or with their phase variant wild-type parents under the conditions of these experiments. Consequently, any differences between their expression profiles cannot be attributed to differences in the rate of growth or cell density. Global differences in their expression profiles were evident: 429 and 379 genes were negatively and positively regulated, respectively, by *rpoN* in the rugose variant compared with the wild-type rugose parent (a complete list is provided in *Supplementary material*, Appendix S8). Similarly, the expression of 424 and 395 genes was negatively and positively regulated, respectively, by *rpoN* in the smooth variant compared with the wild-type smooth parent (a complete list is provided in *Supplementary material*, Appendix S9). Thus, RpoN affects the expression state of genes comprising at least 20% of the genome under this growth condition and a large number of these (584 genes) were regulated similarly in both genetic backgrounds. Below, we focus on subsets of the RpoN-regulated genes that appear to be co-regulated by VpsR or HapR.

As predicted by the postulated role of RpoN in *vps* gene expression that was discussed above, deletion of *rpoN* in the rugose genetic background was found significantly to reduce the expression of genes in *vps* clusters I and II (Fig. 1A–C). However, the magnitude of this effect in *SrpoN* and *RrpoN*, compared with their wild-type parents, was markedly different. In *SrpoN*, expression of the *vpsI* and *vpsII* operon genes was reduced, on average, 2.5- and 1.5-fold, respectively, compared with the wild type. In contrast, expression of *vpsI* and *vpsII* operon genes was reduced, on average, 3.2- and 10-fold in the

RrpoN mutant compared with the rugose variant. For comparative purposes, the average expression of the *vpsI* and *vpsII* operons was five- and 13-fold higher in the rugose variant relative to the smooth variant. We observed previously that expression of the *vpsA* and *vpsL* genes was not altered in the *RrpoN* mutant (Yildiz *et al.*, 2001). Here, we find it to be reduced in the *RrpoN* mutant compared with the rugose variant. We believe that this discrepancy results from differences in the growth state of the samples used for these comparisons. We also determined the average induction of the *vpsI* and *vpsII* operons in the *vpsR* mutants. In the *SvpsR* mutant, *vpsI* and *vpsII* operon gene expression was reduced by 2.56- and 1.58-fold. In contrast, expression was reduced 11- and 20-fold in the *RvpsR* mutant for the *vpsI* and *vpsII* operons. Taken together, these observations show that differences in the regulation of the *vps* operons vary significantly as a function of genetic background. In contrast to its effect on the expression of *vps* genes, the expression of genes encoding the Eps type II secretion apparatus was not altered in the *RrpoN* mutant compared with the wild-type rugose variant. Thus, expression of the type II secretion system that is required for the export of cholera toxin and for the biosynthesis or export of VPS^{EITor} does not require RpoN.

The above-described effect of RpoN on expression of the *vpsI* and *vpsII* operons was associated with delayed development of the corrugated colonial morphotype for *RrpoN* colonies compared with colonies formed by the rugose parent. Moreover, when fully developed, the *RrpoN* colonies were still less corrugated and less compact than the rugose variant. Similarly, under static conditions, the biofilm-forming capacity of the *RrpoN* mutant, assessed by crystal violet staining, was found to be decreased by 3.5-fold relative to the wild-type rugose variant (Fig. 2A). By comparison, the biofilm-forming capacity of the *RvpsR* mutant, under identical conditions, was decreased fivefold. To decipher differences in the contribution of VpsR and RpoN to biofilm structure under non-static conditions, biofilms of the *RvpsR* and *RrpoN* mutants were formed using the flow system described above, and the biofilms were imaged by CSLM (Fig. 2-B) and analysed using COMSTAT (Fig. 2–C) (Heydorn *et al.*, 2000b). The average thickness of *RvpsR* biofilms was found to be significantly lower than that of rugose biofilms. In contrast, both the roughness and the surface to biovolume ratio were higher in *RvpsR* biofilms, an effect that we attribute to the reduced capacity of *RvpsR* to produce extracellular matrix. In turn, this was correlated with a diminished capacity to form the three-dimensional biofilm structures that are typical of the rugose variant (Fig. 2B). Unexpectedly, *RrpoN* biofilms were the thickest of all the biofilms assessed in this study, even thicker than biofilms formed by the rugose parent, reaching a height of 45 µm

(Fig. 2B). Possible explanations for differences in biofilm thickness between the *RpoN* mutant and rugose parent under static (Fig. 2A) and flow (Fig. 2B) conditions include: the accumulation of autoinducers under static but not flow conditions; qualitative differences in VPS^{EITor} composition under the two biofilm conditions; the production of matrix material under flow conditions by genes other than *vpsI* and *vpsII*; and decreased motility of the *RpoN* mutant (Table 1), preventing cells from leaving the biofilm and resulting in the accumulation of cells in the biofilm. One of these possibilities was explored by isolating VPS matrix from the *RpoN* mutant. Analysis of this material showed that it was similar in composition to VPS^{EITor} from the rugose variant, indicating that the observed difference in biofilm thickness between the rugose variant and the *RpoN* mutant was not likely to result from differences in carbohydrate composition. Further analysis of these biofilms showed that surface roughness was similar, but the surface to biovolume ratio was lower for the *RpoN* mutant compared with the rugose variant.

To understand better the contribution of RpoN and VpsR to biofilm formation in *V. cholerae* O1 El Tor, we compared the biofilm-forming properties of the *SvpsR* and *SrpoN* mutants with the wild-type smooth parent under static conditions. As shown in Fig. 2A, this analysis revealed that the biofilm-forming capacity of *SvpsR* is similar to the wild-type smooth variant. This is not an unexpected result because the smooth colonial variant of the strain used in these studies produces very little VPS^{EITor}. As a consequence, even if VpsR is required for the positive regulation of the *vps* genes in the smooth genetic background, such an effect would not be evident owing to the low expression levels of these genes in the wild-type smooth colonial variant under the condition tested. In contrast, the *SrpoN* mutant exhibited a fivefold reduction in biofilm formation compared with the wild-type smooth variant (Fig. 2A). This too was an expected result as RpoN is required for flagellar biogenesis and motility (Klose and Mekalanos, 1998) and, in turn, flagellar motility contributes to the initial stages of biofilm formation (Watnick and Kolter, 1999). VPS production, on the other hand, is believed to contribute to a later stage in biofilm development (Watnick and Kolter, 1999; Yildiz and Schoolnik, 1999). Analysis of *SrpoN* biofilms formed under flow conditions showed them to be less developed, compared with the smooth variant, having a thickness <10 µm (Fig. 2B). *SvpsR* biofilms, on the other hand, were somewhat more developed relative to the wild-type parent. Together, these results show that VpsR is required for the formation of three-dimensional biofilm structures in both genetic backgrounds and that the effect of the RpoN mutation is phase variant dependent.

Transcriptome analysis also showed that *hapR* was induced fivefold in the *rpoN* mutant, suggesting that the

effect of RpoN on the LuxO, HapR regulatory cascade was responsible, at least in part, for the reduced expression of *vps* genes in the *RpoN* mutant. We did not expect to detect a parallel downregulation of VpsR expression in the *rpoN* mutant because RpoN is not predicted to regulate *vpsR* expression, but rather to act in concert with it. LuxO was also reported to increase *V. cholerae* virulence gene expression at low cell densities by repressing the expression of HapR, a negative regulator of TcpP and ToxR regulon expression (Zhu *et al.*, 2002). Thus, if RpoN acts in concert with LuxO, then inactivation of *rpoN* is predicted to relieve LuxO-mediated repression of *hapR*, leading to increased expression of HapR and, hence, to the repression of toxin co-regulated pilus (TCP) biosynthesis genes and genes encoding cholera toxin. The expression profiling results obtained during the course of this study address this hypothesis: the *rpoN* mutant showed reduced levels of expression of *tcpP*, *tcpH* and *tcpA* (Fig. 4A). In contrast, the expression of *ctx* genes was unaltered under the conditions tested. As shown in Fig. 4B, deletion of *rpoN* also led to reduced expression of *rtxA* (VC1451) encoding the RTX toxin and VC1450, which encodes RTX toxin-activating protein (Lin *et al.*, 1999). Thus, like its effect on *vps* gene expression, RpoN seems to be required as an essential cofactor with LuxO for the expression of at least two virulence factors, TCP and the RTX toxin. This defect in TCP expression may account, in part, for the findings of Klose and Mekalanos (1998) that an *rpoN* mutant is more impaired in its ability to colonize the intestine of the suckling mouse than can be accounted for by the loss of RpoN-dependent motility function alone, an effect that was confirmed here by expression profiling experiments that showed dramatic downregulation of flagellar biosynthesis gene expression in the *rpoN* mutants.

The effects of RpoN on *vps* and virulence gene expression discussed above were attributed to its interaction with LuxO and VpsR. However, inspection of the expression profile (Fig. 4C) showed 2.4-fold increased expression of *rpoS* (VC05340) in the *rpoN* mutant, indicating that RpoN normally downregulates *rpoS* expression under this growth condition. As RpoS was found to upregulate *hapR* expression, the inactivation of *rpoN*, by causing increased expression of RpoS and HapR, should reduce the expression *V. cholerae* virulence and *vps* genes – results that were corroborated by the expression profiling results described above. Thus, with respect to its capacity to upregulate *vps* gene expression – a central feature of the rugose colonial morphotype – RpoN potentially acts through the three regulatory pathways depicted in Fig. 5.

Messages for the genes required for transcription functions including VC2467 (RNA polymerase sigma E factor, *rpoE*) and its regulators VC2466 (sigma E negative regu-

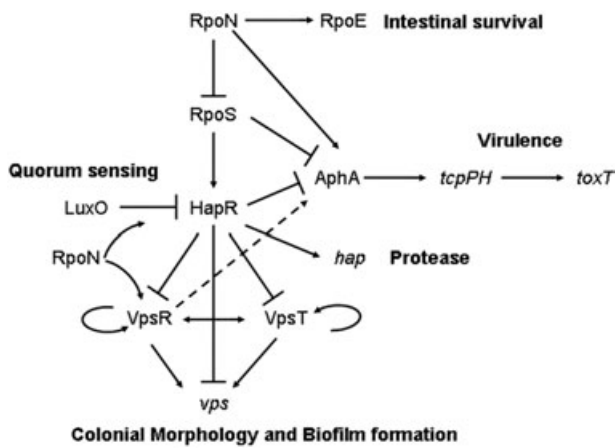


Fig. 5. Regulatory pathways controlling *vps* and virulence gene expression. Whole-genome expression profiling revealed that the transcriptional regulation of *vps* genes and the regulators VpsR and VpsT is negatively controlled by HapR. The expression of *vps* genes is positively controlled by the alternative sigma factor RpoN and negatively regulated by the alternative sigma factor RpoS. Transcription of AphA, a regulator of *tcpPH*, is positively regulated by VpsR and RpoN and negatively regulated by RpoS and HapR. It has yet to be determined whether the control of *vps* and virulence genes by the alternative sigma factors RpoS and RpoN results completely from their action on *hapR* transcription.

latory protein, *rseA*) and VC2465 (sigma E regulatory protein, *rseB*) were reduced in the *rpoN* mutants relative to wild type (Fig. 4C). It has been shown recently that RpoE regulates the expression of virulence genes (Kovacikova and Skorupski, 2002b). It is therefore likely that reduced virulence gene expression in the *rpoN* mutant could also result from reduced RpoE expression. In this study, we also observed that *rpoN* regulates the expression of *rpoS* in a negative manner. Thus, the large differences in the gene expression profiles of the *rpoN* mutant and wild-type parent could be due to changes in sigma factor transcription and, in turn, cellular sigma factor concentrations. In a recent study of *Borrelia burgdorferi*, it was also shown that RpoS and RpoN can directly control the expression of each other (Hubner *et al.*, 2001). Taken together, these results show that sigma factors can regulate each other, an increasingly recognized theme in the regulation of prokaryotic cell physiology.

Message abundance for a large set of genes involved in the transport of nutrients and cations was higher in the *rpoN* mutant. Of particular interest is the derepression of genes encoding for vibriobactin transport including: VC0771 (*vibB*), vibriobactin specific isochorismatase; VC0773 (*vibC*), vibriobactin specific isochorismatase synthase; VC0774 (*vibA*), vibriobactin specific 2,3-dihydro-2,3-dihydroxybenzoate dehydrogenase; VC0775, vibriobactin synthesis protein; VC0776 (*fepB*), ferric vibriobactin ABC transporter; and periplasmic ferric vibriobactin-binding protein.

Chemotaxis-related functions were also found to be regulated by RpoN. Messages for VCA1091 chemotaxis protein methyl transferase CheR (*cheR-3*), VCA1093 purine-binding chemotaxis protein CheW (*cheW-2*), VC1904 purine-binding chemotaxis protein CheW (*cheW-3*), VC1905 chemotaxis protein CheA (*cheA-3*), VCA1906 chemotaxis protein CheY (*cheY-4*) and VC1402 (CheW putative) were higher in the *RrpoN* mutant relative to the wild-type parent. In addition, the expression of nine genes encoding for methyl-accepting chemotaxis proteins (VC0216, VC0282, VC1298, VC1403, VC1643, VCA0031, VCA0658, VCA1034, VCA1069) was increased, and expression of six MCPs (VC1313, VCA0068, VCA0663, VCA0864, VCA0923, VCA0974) was repressed compared with the wild-type parent.

It was of interest that the expression of genes required for 2'-deoxyribonucleotide metabolism (VC1255, VC1256), genes encoding for salvage enzymes (VC1034, VC1231 VC2348, VC2349, VCA0053) and VC2352 encoding for a NupC family protein with nucleoside transport function was increased in the *RrpoN* mutants, indicating that they are normally repressed by the action of RpoN. Intriguingly, expression of genes involved in purine and pyrimidine biosynthesis including VC0986 adenylate kinase (*adk*), VC1038 uridine kinase (*udk*), VC1129 inosine-guanosine kinase (*gsk-1*), VC2708 guanylate kinase (*gmk*), VC0767 inosine-5'-monophosphate dehydrogenase (*guaB*), VC0768 GMP synthase (*guaA*), VC1126 adenylosuccinate lyase (*purB*), VC0211 orotate phosphoribosyltransferase (*pyrE*) and VC1491 dihydroorotate dehydrogenase (*pyrD*) were repressed in the *rpoN* mutant. Thus, results from the study of these *rpoN* mutants demonstrate that an increase in the transcription of nucleoside salvage enzymes is associated with a decrease in the transcription of genes involved in the *de novo* synthesis of nucleotides. Consequently, the cell's ability to co-ordinate these two related metabolic pathways is directly or indirectly regulated by RpoN.

Conclusion

Colony phase variation, a process that generates phenotypically and possibly genotypically diverse populations, is common in bacteria that reside in multiple microenvironments. *V. cholerae* has the capacity to undergo a phase variation event that results in the generation of two morphologically different colony variants. This study has elucidated the molecular consequences of smooth-to-rugose conversion in a *V. cholerae* O1 El Tor clinical isolate. Analysis of these results showed that the expression of phase variation genes was controlled by a complex regulatory circuit that interacts with a regulatory cascade governing virulence gene expression (Fig. 5).

Experimental procedures

Bacterial strains and media

The *V. cholerae* strains used were the smooth and rugose phase variants of A1552 (wild type, El Tor, Inaba and Rif^R) and the *vpsR*, *hapR*, *rpoN* and *rpoS* mutants of these colony phase variants. The *E. coli* strain DH5 α was used for standard DNA manipulation experiments, and the *E. coli* strain S17-1 λ pir was used for conjugation with *V. cholerae*. Bacteria were grown in standard Luria–Bertani (LB) broth with 0.5% NaCl at 30°C. When appropriate, 100 μ g ml⁻¹ ampicillin and 100 μ g ml⁻¹ rifampicin were added to the media.

Mutagenesis and generation of null mutants

To identify possible negative regulators of the rugose colonial morphotype, the smooth variant of *V. cholerae* O1 El Tor strain A1552 was subjected to Tn5 mutagenesis, and mutants capable of forming pellicles and exhibiting rugose colonial morphology were identified. A detailed description of the transposon mutagenesis and generation of the mutants and complementing plasmids is provided in *Supplementary material*, Appendix S13.

RNA isolation

Overnight-grown cultures of *V. cholerae* O1 El Tor in LB medium at 30°C were diluted 1:200 in fresh LB medium incubated at 30°C by shaking (200 r.p.m.) until they reached mid-exponential phase. To ensure homogeneity, exponential phase cultures were diluted 1:100 in fresh LB medium and grown to an OD₆₀₀ of 0.3–0.4. Aliquots (2 ml) were collected by centrifugation for 2 min at room temperature. The cell pellets were immediately resuspended in 1 ml of Trizol reagent (Invitrogen) and stored at –80°C. The total RNA from the pellets and colonies was isolated according to the manufacturer's instructions. To remove contaminating DNA, total RNA was incubated with RNase-free DNase I (Ambion), and the RNeasy Mini kit (Qiagen) was used to clean up RNA after DNase digestion.

cDNA synthesis, microarray hybridization and data analysis

For whole-genome comparisons of exponentially grown cultures, a common reference RNA was prepared from the exponentially grown smooth variant. Equal amounts of RNA from the test samples and reference sample (1.5–3 μ g of total RNA) were labelled by direct incorporation of Cy3-dUTP or Cy5-dUTP (Amersham) in a reverse transcription (RT) reaction as described previously (Schoolnik *et al.*, 2001). The two cDNA pools from both reactions were mixed and purified using microcon 10 units (Amicon). Then, the concentrated reaction mix was applied to the array surface and allowed to hybridize to PCR fragments representing each of the ORFs of the *V. cholerae* O1 El Tor genome at 65°C for 6–20 h. For whole-genome comparison of colonies, RNA from different phase variants and mutants was labelled, and hybridization was performed as described above. After hybridization, the

arrays were washed, dried and scanned using an Axon scanner to measure the fluorescence intensity of each dye in each ORF-specific spot. These fluorescence intensity values were analysed using software provided by the Stanford Microarray Data Base facility to determine normalized signal intensities and signal ratios of the test and experimental samples. To identify significantly regulated genes, these data were further analysed by the SAM (Tusher *et al.*, 2001) method using the following criteria: $\leq 1\%$ false-positive discovery rate and ≥ 1.5 -fold transcript abundance difference between the reference and experimental samples. These data were also analysed by the hierarchical clustering method (Eisen *et al.*, 1998) to identify genes with similar expression patterns using GENESIS software.

Motif analysis of the upstream regions of phase variation-regulated genes

MOTIF REGRESSOR, MDSCAN APPROACH (Liu *et al.*, 2002) and BIOPROSPECTOR (Liu *et al.*, 2001) algorithms were applied to data from the whole-genome expression profiling experiments to look for transcription factor-binding motifs that are involved in regulation. Detailed descriptions of the analyses are provided in *Supplementary material*, Appendix S14.

Biofilm formation

The biofilm-forming capabilities of the smooth and rugose phase variants and the mutant strains were compared by a crystal violet staining assay after 6 h of incubation in polyvinyl chloride microtitre plates under static conditions in LB medium at 30°C (Yildiz and Schoolnik, 1999). For flow cell experiments, biofilms were grown at 30°C in flow chambers with individual channel dimensions of 1 by 4 by 40 mm supplied at a flow of 3 ml h⁻¹ with 50 times diluted LB medium supplemented with 9 g l⁻¹ NaCl. The flow system was assembled and prepared as described previously (Heydorn *et al.*, 2000a). Cultures for inoculation of the flow channels were prepared by inoculating a single colony from a plate into test tubes containing LB medium and growing them at 30°C for 16 h. Cultures were diluted to an optical density at 600 nm of 0.1 in 0.9% NaCl and used for inoculation. A 350 μ l volume of diluted culture was injected into each flow channel with a small syringe. After inoculation, flow channels were left at 30°C for 1 h. Medium flow was then started at a constant rate of 3 ml h⁻¹ with a Watson Marlow 205S peristaltic pump. Images from each experiment were analysed by the computer program COMSTAT (Heydorn *et al.*, 2000b). A fixed threshold value and connected volume filtration were used for all image stacks.

Acknowledgements

We thank members of the Schoolnik laboratory and Yildiz laboratory for their suggestions. We are very grateful to Hakan Ates Gurcan for his help with the data analysis. F.H.Y. is a new scholar in the Ellison Medical Foundation Global Infectious Diseases Program. This work was supported in part by grant RO1-AI43422 from National Institutes of Health.

Supplementary material

The following material is available from
<http://www.blackwellpublishing.com/products/journals/suppmat/mmi/mmi4154/mmi4154sm.htm>

Appendix S1. A complete list of differentially regulated genes between the smooth and rugose phase variants during exponential growth.

Appendix S2. A complete list of differentially regulated genes between the rugose and *RvpsA* mutant during exponential growth.

Appendix S3. A complete list of differentially regulated genes between the smooth and phase variant and *RvpsA* mutant during exponential growth.

Appendix S4. A complete list of differentially regulated genes between the smooth phase variant and *ShapR* mutant during exponential growth.

Appendix S5. A complete list of differentially regulated genes between the smooth phase variant and *SrpoS* mutant during exponential growth.

Appendix S6. A complete list of differentially regulated genes between the rugose phase variant and *RvpsR* mutant during exponential growth.

Appendix S7. A complete list of differentially regulated genes between the smooth phase variant and *SvpsR* mutant during exponential growth.

Appendix S8. A complete list of differentially regulated genes between the rugose phase variant and *RrpoN* mutant during exponential growth.

Appendix S9. A complete list of differentially regulated genes between the smooth phase variant and *SrpoN* mutant during exponential growth.

Appendix S10. List of transcripts with the VC repeated sequence in their upstream regulatory regions.

Appendix S11. HapR sites in *V. cholerae* O1 El Tor genome.

Appendix S12. Computationally derived VpsR binding sites.

Appendix S13. Mutagenesis and generation of null mutants.

Appendix S14. Motif analysis of the upstream regions of phase variation-regulated genes.

References

- Ali, A., Mahmud, Z.H., Morris, J.G., Jr, Sozhamannan, S., and Johnson, J.A. (2000a) Sequence analysis of TnphoA insertion sites in *Vibrio cholerae* mutants defective in rugose polysaccharide production. *Infect Immun* **68**: 6857–6864.
- Ali, A., Johnson, J.A., Franco, A.A., Metzger, D.J., Connell, T.D., Morris, J.G., Jr, and Sozhamannan, S. (2000b) Mutations in the extracellular protein secretion pathway genes (*eps*) interfere with rugose polysaccharide production in and motility of *Vibrio cholerae*. *Infect Immun* **68**: 1967–1974.
- Ali, A., Rashid, M.H., and Karaolis, D.K. (2002) High-frequency rugose exopolysaccharide production by *Vibrio cholerae*. *Appl Environ Microbiol* **68**: 5773–5778.
- Arana, I., Muela, A., Iriberrri, J., Egea, L., and Barcina, I. (1992) Role of hydrogen peroxide in loss of culturability mediated by visible light in *Escherichia coli* in a freshwater ecosystem. *Appl Environ Microbiol* **58**: 3903–3907.
- Casper-Lindley, C., and Yildiz, F.H. (2004) VpsT is a transcriptional regulator required for expression of *vps* biosyn-

- thesis genes and the development of rugose colonial morphology in *Vibrio cholerae* O1 El Tor. *J Bacteriol* **186**: 1574–1578.
- Conlon, E.M., Liu, X.S., Lieb, J.D., and Liu, J.S. (2003) Integrating regulatory motif discovery and genome-wide expression analysis. *Proc Natl Acad Sci USA* **100**: 3339–3344.
- Eisen, M.B., Spellman, P.T., Brown, P.O., and Botstein, D. (1998) Cluster analysis and display of genome-wide expression patterns. *Proc Natl Acad Sci USA* **95**: 14863–14868.
- Faruque, S.M., Albert, M.J., and Mekalanos, J.J. (1998) Epidemiology, genetics, and ecology of toxigenic *Vibrio cholerae*. *Microbiol Mol Biol Rev* **62**: 1301–1314.
- Gosink, K.K., Kobayashi, R., Kawagishi, I., and Hase, C.C. (2002) Analyses of the roles of the three *cheA* homologs in chemotaxis of *Vibrio cholerae*. *J Bacteriol* **184**: 1767–1771.
- Hammer, B.K., and Bassler, B.L. (2003) Quorum sensing controls biofilm formation in *Vibrio cholerae*. *Mol Microbiol* **50**: 101–104.
- Haugo, A.J., and Watnick, P.I. (2002) *Vibrio cholerae* CytR is a repressor of biofilm development. *Mol Microbiol* **45**: 471–483.
- Heidelberg, J.F., Eisen, J.A., Nelson, W.C., Clayton, R.A., Gwinn, M.L., Dodson, R.J., et al. (2000) DNA sequence of both chromosomes of the cholera pathogen *Vibrio cholerae*. *Nature* **406**: 477–483.
- Hengge-Aronis, R. (1993) Survival of hunger and stress: the role of *rpoS* in early stationary phase gene regulation in *E. coli*. *Cell* **72**: 165–168.
- Hengge-Aronis, R. (2002a) Signal transduction and regulatory mechanisms involved in control of the sigma (S) (RpoS) subunit of RNA polymerase. *Microbiol Mol Biol Rev* **66**: 373–395. table of contents.
- Hengge-Aronis, R. (2002b) Recent insights into the general stress response regulatory network in *Escherichia coli*. *J Mol Microbiol Biotechnol* **4**: 341–346.
- Heydorn, A., Ersboll, B.K., Hentzer, M., Parsek, M.R., Givskov, M., and Molin, S. (2000a) Experimental reproducibility in flow-chamber biofilms. *Microbiology* **146**: 2409–2415.
- Heydorn, A., Nielsen, A.T., Hentzer, M., Sternberg, C., Givskov, M., Ersboll, B.K., and Molin, S. (2000b) Quantification of biofilm structures by the novel computer program COMSTAT. *Microbiology* **146** (10): 2395–2407.
- Hubner, A., Yang, X., Nolen, D.M., Popova, T.G., Cabello, F.C., and Norgard, M.V. (2001) Expression of *Borrelia burgdorferi* OspC and DbpA is controlled by a RpoN-RpoS regulatory pathway. *Proc Natl Acad Sci USA* **98**: 12724–12729.
- Islam, M.S., Drasar, B.S., and Sack, R.B. (1993) The aquatic environment as a reservoir of *Vibrio cholerae*: a review. *J Diarrhoeal Dis Res* **11**: 197–206.
- Jansson, P.E., Kenne, L., and Lindberg, B. (1975) Structure of extracellular polysaccharide from *Xanthomonas campestris*. *Carbohydr Res* **45**: 275–282.
- Jobling, M.G., and Holmes, R.K. (1997) Characterization of *hapR*, a positive regulator of the *Vibrio cholerae* HA/protease gene hap, and its identification as a functional homologue of the *Vibrio harveyi luxR* gene. *Mol Microbiol* **26**: 1023–1034.
- Klose, K.E., and Mekalanos, J.J. (1998) Distinct roles of an

- alternative sigma factor during both free-swimming and colonizing phases of the *Vibrio cholerae* pathogenic cycle. *Mol Microbiol* **28**: 501–520.
- Klose, K.E., Novik, V., and Mekalanos, J.J. (1998) Identification of multiple sigma54-dependent transcriptional activators in *Vibrio cholerae*. *J Bacteriol* **180**: 5256–5259.
- Kovacikova, G., and Skorupski, K. (2002a) Regulation of virulence gene expression in *Vibrio cholerae* by quorum sensing: HapR functions at the *aphA* promoter. *Mol Microbiol* **46**: 1135–1147.
- Kovacikova, G., and Skorupski, K. (2002b) The alternative sigma factor sigma (E) plays an important role in intestinal survival and virulence in *Vibrio cholerae*. *Infect Immun* **70**: 5355–5362.
- Kredich, N.M. (1996) Biosynthesis of cysteine. In *Escherichia coli and Salmonella: Cellular and Molecular Biology*, Vol. I. Neidhardt, N.C. (ed.). Washington, DC: American Society for Microbiology Press, pp. 514–527.
- Lin, W., Fullner, K.J., Clayton, R., Sexton, J.A., Rogers, M.B., Callia, K.E., et al. (1999) Identification of a *Vibrio cholerae* RTX toxin gene cluster that is tightly linked to the cholera toxin prophage. *Proc Natl Acad Sci USA* **96**: 1071–1076.
- Liu, X., Brutlag, D.L., and Liu, J.S. (2001) BioProspector: discovering conserved DNA motifs in upstream regulatory regions of co-expressed genes. *Pac Symp Biocomput* 127–138.
- Liu, X.S., Brutlag, D.L., and Liu, J.S. (2002) An algorithm for finding protein-DNA binding sites with applications to chromatin-immunoprecipitation microarray experiments. *Nature Biotechnol* **20**: 835–839.
- Mazel, D., Dychinco, B., Webb, V.A., and Davies, J. (1998) A distinctive class of integron in the *Vibrio cholerae* genome. *Science* **280**: 605–608.
- Meibom, K.L., Li, X.B., Nielsen, A.T., Wu, C.Y., Roseman, S., and Schoolnik, G.K. (2004) The *Vibrio cholerae* chitin utilization program. *Proc Natl Acad Sci USA* **101**: 2524–2529.
- Morris, J.G., Jr, Sztein, M.B., Rice, E.W., Nataro, J.P., Losonsky, G.A., Panigrahi, P., et al. (1996) *Vibrio cholerae* O1 can assume a chlorine-resistant rugose survival form that is virulent for humans. *J Infect Dis* **174**: 1364–1368.
- Nesper, J., Lauriano, C.M., Klose, K.E., Kapfhammer, D., Kraiss, A., and Reidl, J. (2001) Characterization of *Vibrio cholerae* O1 El Tor *galU* and *galE* mutants: influence on lipopolysaccharide structure, colonization, and biofilm formation. *Infect Immun* **69**: 435–445.
- North, A.K., Weiss, D.S., Suzuki, H., Flashner, Y., and Kustu, S. (1996) Repressor forms of the enhancer-binding protein NrtC: some fail in coupling ATP hydrolysis to open complex formation by sigma 54-holoenzyme. *J Mol Biol* **260**: 317–331.
- Prouty, M.G., Correa, N.E., and Klose, K.E. (2001) The novel sigma54- and sigma28-dependent flagellar gene transcription hierarchy of *Vibrio cholerae*. *Mol Microbiol* **39**: 1595–1609.
- Rice, E.W., Johnson, C.J., Clark, R.M., Fox, K.R., Reasoner, D.J., Dunnigan, M.E., et al. (1992) Chlorine and survival of 'rugose' *Vibrio cholerae*. *Lancet* **340**: 740.
- Rosenberg, M., and Doyle, R.J. (1990) *Microbial Cell Surface Hydrophobicity*. Washington, DC: American Society for Microbiology Press.
- Rowe-Magnus, D.A., Guerout, A.M., Ploncard, P., Dychinco, B., Davies, J., and Mazel, D. (2001) The evolutionary history of chromosomal super-integrations provides an ancestry for multiresistant integrons. *Proc Natl Acad Sci USA* **98**: 652–657.
- Sandkvist, M. (2001a) Type II secretion and pathogenesis. *Infect Immun* **69**: 3523–3535.
- Sandkvist, M. (2001b) Biology of type II secretion. *Mol Microbiol* **40**: 271–283.
- Schauder, S., Shokat, K., Surette, M.G., and Bassler, B.L. (2001) The LuxS family of bacterial autoinducers: biosynthesis of a novel quorum-sensing signal molecule. *Mol Microbiol* **41**: 463–476.
- Schoolnik, G.K., Voskuil, M.I., Schnappinger, D., Yildiz, F.H., Meibom, K., Dolganov, N.A., et al. (2001) Whole genome DNA microarray expression analysis of biofilm development by *Vibrio cholerae* O1, E1 Tor. *Methods Enzymol* **336**: 3–18.
- Tusher, V.G., Tibshirani, R., and Chu, G. (2001) Significance analysis of microarrays applied to the ionizing radiation response. *Proc Natl Acad Sci USA* **98**: 5116–5121.
- Wai, S.N., Mizunoe, Y., Takade, A., Kawabata, S.I., and Yoshida, S.I. (1998) *Vibrio cholerae* O1 strain TSI-4 produces the exopolysaccharide materials that determine colony morphology, stress resistance, and biofilm formation. *Appl Environ Microbiol* **64**: 3648–3655.
- Watnick, P.I., and Kolter, R. (1999) Steps in the development of a *Vibrio cholerae* El Tor biofilm. *Mol Microbiol* **34**: 586–595.
- Watnick, P.I., Lauriano, C.M., Klose, K.E., Croal, L., and Kolter, R. (2001) The absence of a flagellum leads to altered colony morphology, biofilm development and virulence in *Vibrio cholerae* O139. *Mol Microbiol* **39**: 223–235.
- White, B.P. (1938) The rugose variant of *Vibrios*. *J Pathol* **46**: 1–6.
- Yildiz, F.H., and Schoolnik, G.K. (1998) Role of *rpoS* in stress survival and virulence of *Vibrio cholerae*. *J Bacteriol* **180**: 773–784.
- Yildiz, F.H., and Schoolnik, G.K. (1999) *Vibrio cholerae* O1 El Tor: identification of a gene cluster required for the rugose colony type, exopolysaccharide production, chlorine resistance, and biofilm formation. *Proc Natl Acad Sci USA* **96**: 4028–4033.
- Yildiz, F.H., Dolganov, N.A., and Schoolnik, G.K. (2001) VpsR, a member of the response regulators of the two-component regulatory systems, is required for expression of *vps* biosynthesis genes and EPS (ETr)-associated phenotypes in *Vibrio cholerae* O1 El Tor. *J Bacteriol* **183**: 1716–1726.
- Zalkin, H., and Nygaard, P. (1996) Biosynthesis of purine nucleotides. In *Escherichia coli and Salmonella: Cellular and Molecular Biology*, Vol. I. Neidhardt, N.C. (ed.). Washington, DC: American Society for Microbiology Press, pp. 561–579.
- Zhu, J., and Mekalanos, J.J. (2003) Quorum sensing-dependent biofilms enhance colonization in *Vibrio cholerae*. *Dev Cell* **5**: 647–656.
- Zhu, J., Miller, M.B., Vance, R.E., Dziejman, M., Bassler, B.L., and Mekalanos, J.J. (2002) Quorum-sensing regulators control virulence gene expression in *Vibrio cholerae*. *Proc Natl Acad Sci USA* **99**: 3129–3134.